

HIGH RESOLUTION NEAR-EDGE SPECTROSCOPY OF MOLECULES AND MOLECULAR VAN DER WAALS CLUSTERS

R. FLESCH, W. TAPPE and E. RÜHL

*Fachbereich Physik, Universität Osnabrück, Barbarastr. 7,
49069 Osnabrück, Germany*

A. A. PAVLYCHEV

*St. Petersburg State University, St. Petersburg 198904,
Russian Federation*

High resolution near-edge excitation of isolated molecules and homogeneous molecular van der Waals clusters is reported. Resonant excitation near the element K-edges of isolated and clustered carbon monoxide and nitrogen gives rise to small spectral shifts that can only be detected by high spectral resolution. The experimental results indicate for the vibrationally resolved $1s \rightarrow \pi^*$ transitions of isolated molecules that symmetric line shapes cannot be used rather than the lifetime-broadened rotational fine structure. Clustered molecules exhibit characteristic redshifts of the order of a few meV relative to the corresponding isolated molecules. Changes in Franck–Condon factors and changes in spectral line shape are observed, as well. The experimental results are discussed in the framework of the quasiatomic approach with respect to intermolecular interactions and dynamic localization of resonant core-to-valence excitations.

1. Introduction

Clusters bridge the gap between the gas and the condensed phase of matter.¹ Core level excitation of clusters has recently become a field of research which has been shown to provide unique information on size effects of matter by element- and site-selective excitation.^{2–4} Synchrotron radiation is the most suitable radiation source for such experiments,⁵ where excitation in the near-edge regime allows one to probe sensitively size- and composition-dependent changes in electronic structure of variable size atomic clusters.^{6–8} Size-dependent changes in electronic structure occur in atomic clusters as a result of the conversion of atomic Rydberg states into the corresponding surface and bulk excitons of the solid. Gas-to-solid shifts have been investigated for various simple model systems, such as rare gases.⁹ These are typically of the order of a few hundred meV, so that gas-to-solid shifts are easily detected even by low resolution soft X-rays.^{2,10} More recently, high resolution near-edge spectroscopy of variable size krypton clusters has revealed small spectral shifts that are as small as 20 meV.⁸ Various blueshifted features were

assigned to excitations of different geometric sites in clusters, such as corners, edges, faces, and subsurface layers. This work gave evidence for the fact that the geometric structures of the clusters are fairly imperfect, since edge sites dominate the small cluster regime. This result is in general agreement with earlier results from EXAFS spectroscopy, where it was found that small imperfectly shaped clusters give rise preferentially to fcc moieties in the size regime above 200 atoms per cluster.¹¹ These are evidently faster growing in a jet expansion than icosahedra,¹² which are known to dominate the small cluster regime.¹³

Size effects in molecular cluster systems have been investigated in the core excitation regime. First studies made use of low energy resolution of the monochromatic synchrotron radiation ($E/\Delta E \leq 500$).¹⁴ The core-to-valence transitions of gas phase molecules and their clusters occurring in the pre-edge regime are almost identical in energy, so that hardly any changes in electronic structure were observed.¹⁴ Later work employed medium energy resolution ($500 \leq E/\Delta E \leq 5000$) in the soft X-ray regime. Size-dependent changes in electronic structure were only observed in cluster systems with strong chemical

or intermolecular bonds, for example in variable size sulfur¹⁵ and water clusters.¹⁶

More recently, substantial blueshifts of the order of 1 eV relative to the isolated molecule were found for the $1s \rightarrow \sigma^*$ shape-resonance regime in nitrogen clusters and solid nitrogen.¹⁷ These results were rationalized in terms of the quasiatomic approach (QA)¹⁸ by considering the effect of the low symmetric cluster field on strongly localized molecular excitations with respect to their dynamic symmetry.^{17,19} First results from high resolution near-edge spectroscopy gave evidence for small spectral shifts which are of the order of a few meV. These were observed for $1s \rightarrow \pi^*$ -excited molecular clusters.^{20,21}

We focus in this paper on new aspects that are related to high resolution near-edge excitation of variable size molecular van der Waals clusters. We discuss spectral line shapes of vibrationally resolved $1s \rightarrow \pi^*$ bands of molecular and clustered nitrogen and carbon monoxide, changes in Franck–Condon factors, and suitable assignments of spectral shifts that occur upon cluster formation.

2. Experimental

The experimental setup has been described earlier in detail.¹⁴ Briefly, a continuous supersonic jet expansion is used for cluster production, where pure molecular gases are expanded through a 50 μm nozzle. The cluster jet is shaped by a 500 μm skimmer. It is excited by monochromatic synchrotron radiation from the storage ring BESSY-II (Berlin, Germany). The experiments were carried out at the U49-SGM-1 beam line where an energy resolution $E/\Delta E > 10^4$ is reached in the soft X-ray regime.²² The cluster jet is crossed by the beam of monochromatic synchrotron radiation under collision free conditions in the ionization region of a time-of-flight mass spectrometer (TOF-MS). This device is used in a pulsed mode in order to separate and detect the cluster cations and their fragments. Yields of mass-selected cations are obtained by selecting a mass channel while scanning the photon energy. The spectra are normalized to the photon flux by using either the photocurrent of a gold mesh or the total ion yield of rare gases. The photon energy scale is calibrated by comparison with high resolution electron energy loss data.²³

Variable size clusters are formed under the following conditions, where the stagnation pressure p_0 and stagnation temperature T_0 are varied in the following

regimes: $1 \text{ bar} \leq p_0 \leq 5 \text{ bar}$ and $150 \text{ K} \leq T_0 \leq 300 \text{ K}$, leading at low T_0 and high p_0 to the efficient formation of clusters. The average cluster size $\langle N \rangle$ characterizes the size distribution of the neutral cluster jet. In the case of CO and N_2 clusters, one obtains $\langle N \rangle \leq 150$ under the present expansion conditions (cf. Ref. 24). The gases were of commercial quality (Messer-Griesheim; purity > 99.99%).

3. Results and Discussion

3.1. *C 1s-excited carbon monoxide*

Figure 1 shows a comparison between low and high resolution excitation near the $\text{C } 1s \rightarrow \pi^*$ excitation of CO that was introduced in an effusive jet at room temperature. Curve (a) is the result from standard low resolution work, as obtained recently from second generation storage ring facilities.¹⁷ Curve (b) is obtained from present high resolution work, where the vibrational levels, corresponding to excitations into the $v' = 0$ ($E = 287.400 \text{ eV}$) and $v' = 1$ level ($E = 287.656 \text{ eV}$), respectively. The $v' = 2$ level is weak in intensity. The energy positions and Franck–Condon factors are in agreement with earlier work (cf. Refs. 25 and 26). Typically, the vibrational components can be deconvoluted by using

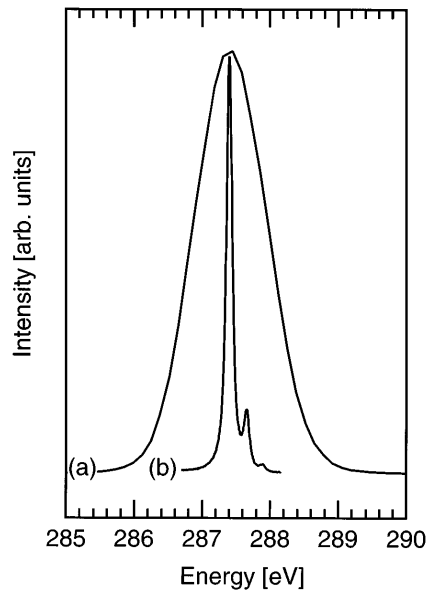


Fig. 1. Total cation yield of carbon monoxide in the regime of the $\text{C } 1s \rightarrow \pi^*$ excitation: (a) low energy resolution (cf. Ref. 17); (b) high energy resolution with evidence for vibrational fine structure.

Voigt profiles into the vibrational components, where the Lorentzian width is due to the considerable lifetime broadening, whereas the Gaussian contribution is essentially the result of the limited energy resolution of the soft X-ray monochromator.⁵ The spectral line shape of the molecular C $1s \rightarrow \pi^*$ ($v' = 0$) transition is approximated by a Lorentzian line width of 85 ± 1 meV and a Gaussian width of 41 ± 1 meV. Both contributions yield the total width of the Voigt profile of 102 ± 1 meV in FWHM. These results are in good agreement with recent work, where the same Lorentzian width was found.²⁶ However, the Gaussian contribution was 54 meV, which is mostly due to an enhanced bandwidth of the X-ray monochromator that was used in previous work. Other recent work has revealed a Lorentzian width of 79 ± 5 meV, where a Gaussian width of 25 ± 5 meV was obtained.²⁷ The spectral line shape also contains a minor asymmetry, where the cation intensity is slightly increased at the low energy part of the line profile. This is most likely an indication for asymmetric broadening effects that are due to thermal excitation of molecular rotations of the room temperature gas. Figure 2 shows in greater detail the influence of thermal excitation of molecular rotations on the spectral line shape of the

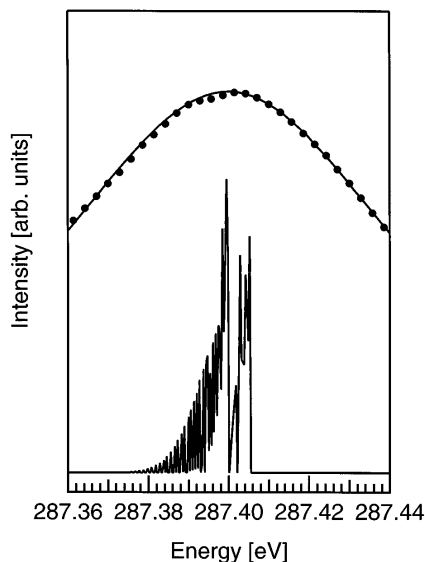


Fig. 2. The influence of rotational broadening on the line shape of the C $1s \rightarrow \pi^*$ ($v' = 0$) transition. The top part shows the experimental data (full points) along with the Voigt-broadened rotational profiles. The bottom part shows the rotational fine structure that is populated upon thermal excitation at $T = 300$ K.

C $1s \rightarrow \pi^*$ ($v' = 0$) excitation, using the well-known molecular constants.²⁸ The 0 K gas is expected to give rise to a single transition from the $J = 0$ level, so that the band is symmetrically broadened. Thermal excitation will result in a somewhat asymmetric distribution of the rotational levels that are spread over ≈ 30 meV at $T = 300$ K. The R branch gives rise to a band head structure at 287.405 eV, whereas the Q branch is located near the center of the band. The P branch stretches out to lower energy, reaching 287.375 eV. Broadening of each rotational line by a 85 meV Lorentzian and a Gaussian width of 41 meV gives excellent agreement with the experimental results. Evidently, the Voigt-broadened rotational fine structure of the thermal gas represents the primary reason for the occurrence of the slight asymmetry of the experimental C $1s \rightarrow \pi^*$ ($v' = 0$) line shape. We note that the difference in line shape between the 300 K gas and the jet-cooled molecule is quite small, if clusters are present in the jet. This is mostly due to the fact that jet cooling yields a rotational temperature that is well above 0 K, since the rotational degrees of freedom are less efficiently cooled than the translational degrees of freedom.²⁹ Moreover, efficient cooling of carbon monoxide is accompanied by spontaneous nucleation so that the molecules are heated. We also note that cooling of molecular rotations yields a slight blueshift of the center of the band, which is of the order of 2 meV when the room temperature gas is compared to the 0 K sample. This slight thermal shift will be discussed below in the context of cluster formation.

3.2. C $1s$ -excited carbon monoxide clusters

The spectral shape of the C $1s \rightarrow \pi^*$ transition of clusters is obtained from the $(\text{CO})_2^+$ yield (cf. Fig. 3), which contains contributions from heavier clusters via fragmentation. It is remarkably similar to that of the isolated molecule, which is simultaneously measured under entirely identical conditions by recording the O^+ yield. This allows us to identify small spectral shifts that can be as small as 1 meV (cf. Ref. 20). The Franck–Condon factors are essentially unchanged when the two spectra are compared to each other. This is an indication for the fact that the C $1s \rightarrow \pi^*$ transition is primarily governed by intramolecular properties rather than by

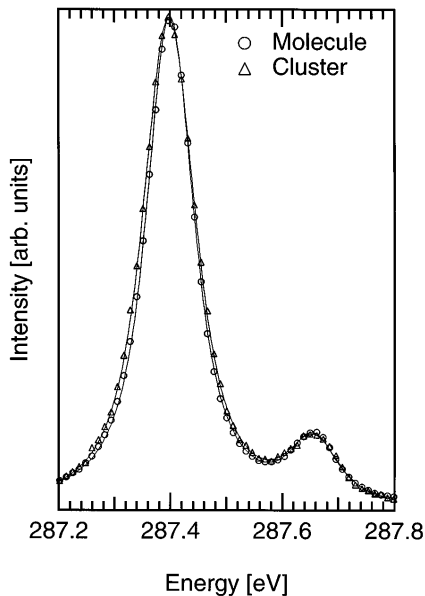


Fig. 3. Photoion yields of O^+ (molecule) and $(\text{CO})_2^+$ (cluster) recorded at $\langle N \rangle \approx 150$. See text for further details.

intermolecular interactions. However, there are small but characteristic differences between the $\text{C } 1s \rightarrow \pi^*$ transitions in molecules and clusters. The $(\text{CO})_2^+$ yield shows a characteristically broadened $\text{C } 1s \rightarrow \pi^*$ ($v' = 0$) transition, where 113 ± 1 meV are found in FWHM (cf. Fig. 3). It is somewhat broader than the molecular transition (102 ± 1 meV). The band can be approximated by a Voigt profile, however, the Lorentzian and Gaussian line widths are slightly increased to 90 ± 1 meV and 50 ± 1 meV, respectively. This cannot be the result of an increased spectral bandwidth of the monochromator. We rather assume that there are other contributions to changes in spectral line shape of clusters that are related to the occurrence of intermolecular vibrations.³⁰ In addition, we observe a small but clearly identifiable redshift of 2 ± 1 meV of the maximum of the $\text{C } 1s \rightarrow \pi^*$ ($v' = 0$) transition in clusters relative to the bare molecule. This spectral redshift can be as large as 4 ± 1 meV if molecular rotations are considered to be entirely frozen (see Subsec. 3.1). The origin of these spectral shifts is discussed in Subsec. 3.4.

3.3. N $1s$ -excited nitrogen clusters

Figure 4 shows a portion of the vibrationally resolved $\text{N } 1s \rightarrow \pi^*$ ($v' = 0, 1$) transition of molecular and

clustered nitrogen. The entire band consists of a Franck–Condon progression that extends to $v' = 6$.²¹ A comparison between the pure gas and clusters indicates that there are only small, but distinct, differences between the two spectra. These include a small redshift of the $\text{N } 1s \rightarrow \pi^*$ transition of clusters relative to the bare molecule as well as small changes in Franck–Condon factors, where the intensity of the levels $v' > 0$ is slightly reduced relative to the vibrational ground state ($v' = 0$) level. We do not observe any spectral broadening in clusters relative to the isolated molecule, which is unlike the results on CO clusters. Various possible origins of the redshift have been discussed recently.²¹ Similar to the results on CO , freezing of molecular rotations can also lead to a small blueshift rather than to a redshift. As a result, this cannot be the origin of the redshift that is shown in Fig. 4. Similarly, changes in intramolecular bonding were discounted.²¹ It was rather assumed that intermolecular vibrations are the origin of the redshift along with dynamic localization, as will be outlined in Subsec. 3.4.

Changes in the relative intensities of the bands within the $1s \rightarrow \pi^*$ progression are assumed to be governed by changes in local geometry of the core-excited molecules that are bound in clusters. Thus, the relative enhancement of the $v' = 0$ level in clusters is rationalized by a decrease of the intramolecular equilibrium distance r_e upon $\text{N } 1s$ excitation. Changes in Franck–Condon factors in clusters are modeled by using a Morse potential energy function for the $^1\Sigma_g^+$ ground state and the core-excited $\text{N } 1s \rightarrow \pi^*$ state, similar to earlier work on the isolated molecule (cf. e.g. Ref. 31). The observed vibrational

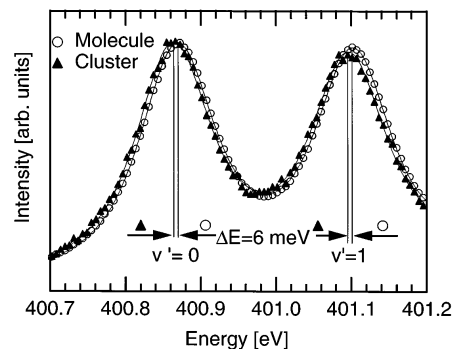


Fig. 4. Photoion yields of N^+ (molecule, open circles) and $(\text{N}_2)_2^+$ (cluster, solid triangles) recorded at $\langle N \rangle \approx 150$. See text for further details.

constant ($\omega_e = 235.2 \text{ cm}^{-1}$) and anharmonicity constant ($\omega_e x_e = 1.9 \text{ cm}^{-1}$) are used to construct the Morse function of the excited state. The overlap integrals of the corresponding wave functions are evaluated numerically. The ground state equilibrium geometry and vibrational constants are taken from Ref. 28.

Slight variations of the excited-state N \equiv N distance change significantly the intensities of the vibrational bands (see Fig. 5). A variety of excited-state N \equiv N distances were used for the Franck–Condon calculations, ranging from $1.170 \text{ \AA} \leq r_e \leq 1.160 \text{ \AA}$. Best agreement with the experimental results on clusters is obtained if the intramolecular N \equiv N distance is slightly reduced by $\sim 100 \text{ fm}$ relative to that in the bare molecule (cf. Fig. 4 and Ref. 21), yielding for clustered nitrogen $r_e = 1.164 \text{ \AA}$. This indicates that the strength of the intramolecular bond is slightly enhanced in $1s$ -excited nitrogen clusters.

3.4. Origin of spectral shifts in core-excited clusters

The changes in spectral linewidths and energy positions upon clustering are rationalized, as follows: The increased Lorentzian linewidths that were found in CO clusters are unlikely to be the result of changes

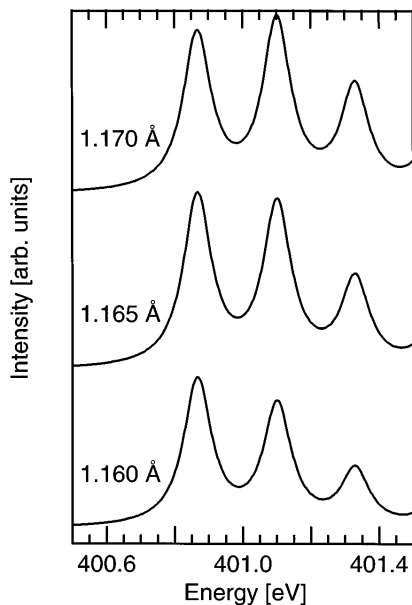


Fig. 5. Calculated Franck–Condon structure of the vibrationally resolved N $1s \rightarrow \pi^*$ transition at different intramolecular N \equiv N bond lengths.

in the core hole lifetime. It is rather expected that they are efficiently affected by fast cluster decay dynamics of the final states that are accessed in clusters due to the intermolecular co-ordinate and partially by the presence of intermolecular vibrations Ω_N . At $N \rightarrow \infty$ it approaches the conventional picture of Gaussian broadening of X-ray transitions in solids with the standard deviation $\sigma = [S(\Omega)\cotan(\Omega/kT)]^{1/2}$, where the coupling constant S is equal to mean number of phonons Ω created in the transition, k is the Boltzmann constant, and T is the absolute temperature. The increase of the Gaussian width by $\approx 20\%$ gives evidence for phonon-like broadening in clusters. In general, X-ray transitions in clusters are strongly localized within the excited molecule so that the spectral shift can either be assigned to efficient freezing of molecular rotations or a polaron-like shift of the Frank–Condon transition in defect centers. A polaron-like shift can also account for dynamic stabilization, corresponding to a spectral redshift, of a core-excited molecule in a cluster.²¹ This effect results from self-trapping in displaced positions off the equilibrium position in a shallow intermolecular potential of a deformable cluster. This is due to changes in the radius of interaction between the core-excited molecule and its neighbors in clusters and in the solid. Hence, an increase in dynamic stabilization on intramolecular vibrational bands (librations) is expected to occur if the interaction of the core-excited molecule with its neighbors increases. The present results on $1s$ -excited N_2 clusters give evidence for strong dynamic localization of the core hole in one of the equivalent atomic sites, since the dynamic dipole moment of N_2^* will dominate the interaction with its neighbors.²¹ The magnitude of the redshift is expected to be related to stabilization that occurs via excitation of librations. In the case of CO clusters there are no equivalent atomic sites so that stabilization is expected to be negligible, resulting in a smaller redshift of the $1s \rightarrow \pi^*$ transition than in N_2 clusters.

4. Conclusion

High resolution near-edge spectroscopy of isolated molecules gives first evidence for the influence of rotational fine structure on spectral line shapes, as evidenced from the analysis of the C $1s \rightarrow \pi^*$ ($v' = 0$) transition of CO. Free clusters reveal small

spectral shifts relative to the isolated molecules. The determination of such spectral shifts will be of importance to determining reliably gas-to-solid shifts, size effects in electronic and geometric structure including dynamic properties of variable size matter. We observe both initial and final state effects on the vibrationally resolved core-to-valence bands in the near-edge regime. These are most likely due to (i) freezing of molecular rotations upon condensation and (ii) stabilization of molecular librations in intermediate core-excited states.

Acknowledgments

Financial support by the Deutsche Forschungsgemeinschaft and by the Fonds der Chemischen Industrie are gratefully acknowledged.

References

1. H. Haberland, *Clusters of Atoms and Molecules*, Vols. 1 and 2 (Springer, Berlin, 1994).
2. E. Rühl, C. Schmale, A. P. Hitchcock and H. Baumgärtel, *J. Chem. Phys.* **98**, 2653 (1993).
3. F. Federmann, O. Björneholm, A. Beutler and T. Möller, *Phys. Rev. Lett.* **73**, 1549 (1994).
4. E. Rühl, in *Theory and Experiments on Clusters*, ed. T. Kodow (World Scientific, Singapore, 2001).
5. J. Stöhr, *NEXAFS Spectroscopy* (Springer, Berlin, 1992).
6. A. A. Pavlychev, E. V. Semenova, A. P. Hitchcock and E. Rühl, *Physica* **208&209**, 187 (1995).
7. O. Björneholm, F. Federmann, F. Fössing and T. Möller, *Phys. Rev. Lett.* **74**, 3017 (1995).
8. A. Knop, B. Wassermann and E. Rühl, *Phys. Rev. Lett.* **80**, 2302 (1998).
9. R. Haensel, N. Kosuch, U. Nielsen, U. Rössler and B. Sonntag, *Phys. Rev.* **B7**, 1577 (1973).
10. A. Knop and E. Rühl, in *Structures and Dynamics of Free Clusters*, eds. T. Kondow, K. Kaya and A. Terasaki (Universal Academy Press, Tokyo, 1996), p. 235.
11. S. Kakar, O. Björneholm, L. Weigelt, A. R. B. de Castro, L. Tröger, R. Frahm, T. Möller, A. Knop and E. Rühl, *Phys. Rev. Lett.* **78**, 1675 (1997).
12. B. W. van de Waal, *Z. Phys.* **D20**, 349 (1991); *Phys. Rev. Lett.* **76**, 1083 (1996).
13. M. R. Hoare, *Adv. Chem. Phys.* **40**, 49 (1979).
14. E. Rühl, *Ber. Bunsenges. Phys. Chem.* **96**, 1172 (1992).
15. C.-M. Teodorescu, D. Gravel and E. Rühl, *J. Chem. Phys.* **109**, 9280 (1998).
16. O. Björneholm, F. Federmann and T. Möller, *J. Chem. Phys.* **111**, 546 (1999).
17. A. A. Pavlychev and E. Rühl, *J. Electron Spectrosc. Relat. Phenom.* **106**, 207 (2000); **107**, 203 (2000).
18. A. A. Pavlychev, A. S. Vinogradov, A. P. Stepanov and A. S. Shulakov, *Opt. Spectrosc.* **75**, 327 (1993).
19. A. A. Pavlychev, N. G. Fominykh, N. Watanabe, K. Sojiima, E. Shigemasa and A. Yagashita, *Phys. Rev. Lett.* **81**, 3623 (1998).
20. E. Rühl, R. Flesch, W. Tappe and A. A. Pavlychev, *J. Synchrotron Radiat.* **8**, 154 (2001).
21. R. Flesch, A. A. Pavlychev, J. J. Neville, J. Blumberg, M. Kuhlmann, W. Tappe, F. Senf, O. Schwarzkopf, A. P. Hitchcock and E. Rühl, *Phys. Rev. Lett.* **86**, 3767 (2001).
22. F. Senf, F. Eggenstein, J. Feikes, R. Follath, S. Hartlaub, T. Knuth, H. Lammert, T. Noll, J. S. Schmidt, G. Reichardt, O. Schwarzkopf, M. Weiss, T. Zeschke and W. Gudat, *Annual Report (BESSY, Berlin, 1999)*, p. 512.
23. A. P. Hitchcock and D. C. Mancini, *J. Electron Spectrosc. Relat. Phenom.* **67**, 1 (1994).
24. A. A. Vostrikov, D. Y. Dubov and I. V. Samoilov, *Tech. Phys.* **39**, 1267 (1994).
25. R. N. S. Sodhi and C. E. Brion, *J. Electron Spectrosc. Relat. Phenom.* **34**, 363 (1984).
26. L. Floreano, G. Natello, D. Cvetko, R. Gotter, M. Malvezzi, L. Marassi, A. Morgante, A. Santinello, A. Verdini, F. Tommasini and G. Tondello, *Rev. Sci. Instrum.* **70**, 3855 (1999).
27. K. C. Prince, M. Vondracek, J. Karvonen, M. Coreno, R. Camilloni, L. Avaldi and M. de Simone, *J. Electron Spectrosc. Relat. Phenom.* **101–103**, 141 (1999).
28. K. P. Huber and G. Herzberg, *Molecular Spectra and Molecular Structure*, Vol. 4 (Van Nostrand, New York, 1979).
29. J. B. Anderson, in *Molecular Beams and Low Density Gas Dynamics*, ed. P. Wegener (Marcel Dekker, New York, 1966).
30. A. Anderson, T. S. Sun and M. C. A. Donkersloot, *Can. J. Phys.* **48**, 2265 (1970).
31. C. T. Chen, Y. Ma and F. Sette, *Phys. Rev.* **A40**, 6737 (1989).